Electro-optical studies of a soluble conjugated polymer with particularly low intrachain disorder

M. G. Harrison, S. Möller, G. Weiser, G. Urbasch, R. F. Mahrt, and H. Bässler
Institute of Physical Chemistry, Department of Physics and Centre for Materials Science, Philipps University of Marburg, D-35032 Marburg, Germany

U. Scherf
Max-Planck Institute for Polymer Research, Ackermannweg 10, D-55128 Mainz, Germany
(Received 1 December 1998; revised manuscript received 22 February 1999)

In contrast with many soluble conjugated polymers, the absorption and electroabsorption spectra of the methyl-substituted ladder-type poly(para-phenylene) show particularly well-resolved excitonic transitions, whose linewidth approaches the narrow values previously only associated with single crystals or isolated chains of polydiacetylenes. At least two distinct vibrational modes couple strongly to the electronic transitions. The electroabsorption spectrum increases quadratically with the electric-field strength, and closely follows the first derivative of absorption throughout most of the visible and near-ultraviolet range, indicative of a quadratic Stark shift of the $1B_u$ singlet exciton. In the region 3.2–3.6 eV, the agreement between the electroabsorption spectrum and the first derivative is offset by a broader spectral feature, which does not correspond to any feature in the linear absorption spectrum. Two-photon fluorescence excitation spectroscopy identifies this state as a forbidden exciton (mA_g), located 0.7 eV above the lowest singlet exciton ($1B_u$). A polarizability of 2060 Å^3 and a dipole moment of 7.17eÅ (34D) is calculated for the $1B_u$ singlet exciton. The spectra show evidence of a small increase of the vibrational frequencies as the polarization of the π system increases. [S0163-1829(99)14835-5]

I. INTRODUCTION

The absorption and electroabsorption spectra of many soluble conjugated polymers show very little sharp structure, and instead show broad bands rather than the narrow electronic transitions usually associated with well-defined discrete molecules. This, together with the apparent coincidence of the (extrinsic) photocurrent threshold and absorption edge, led to the suggestion that the electronic structure of conjugated molecules could be understood within the framework of a one-dimensional semiconductor band model, considering strong electron-phonon coupling but largely neglecting electron-electron interactions. Upon closer examination, particularly with the use of site-selective photoluminescence measurements,[1–3] studies on monodisperse oligomers of the parent polymers and also studies of polymers with higher structural order,[3,4] it became apparent that rather than corresponding to absorption into a one-dimensional semiconductor band, the inhomogenously broadened absorption spectra actually reflect a convolution of sharp molecular excitonic spectra of an ensemble of oligomeric segments within a polymer chain, between which the π conjugation is interrupted by physical or chemical defects such as kinks and twists, saturated sp^3-type tetrahedrally coordinated carbon atoms, or photooxidation defects. The distribution of effective conjugation lengths results in an inhomogeneously broadened distribution of transition energies, which for many soluble conjugated polymers largely obscures the otherwise sharp excitonic structure in the optical spectra, unless site-selective measurements are made.

The magnitude of the binding energy and spatial extent of the lowest allowed singlet exciton ($1B_u$) in conjugated polymers has been the subject of intense debate in recent years. Only for well-ordered polydiacetylenes has it been possible to identify the signature of the continuum unambiguously[5] (Franz-Keldysh oscillations), and to determine for this material an exciton binding energy of around 0.5 eV, which indicates that electron-electron interactions are as important as electron-phonon interactions in calculations of the electronic structure. Admittedly, the chemical structure and morphology of polydiacetylene is quite different from that of poly (*p*-phenylenevinylene) (PPV), since polydiacetylene contains no aromatic rings in the main chain and can form single crystals in which the separation between one-dimensional chains, for example by the urethane side-chains in the case of 4-BCMU or 3-BCMU, is much greater than the interchain separation within PPV chains 4-BCMU and 3-BCMU refer to dacetylene monomers of the formula R-C≡C-C≡C-R, where R is $(CH_2)n$-OCO-NH-CH_2-COO-C_4H_9 and $n=3$ or 4.

The polymer investigated in this study is a methyl-substituted ladder-type poly(para-phenylene) in which the phenylene rings are locked into a rigid, almost planar conformation by the methylene bridges. The structural formula

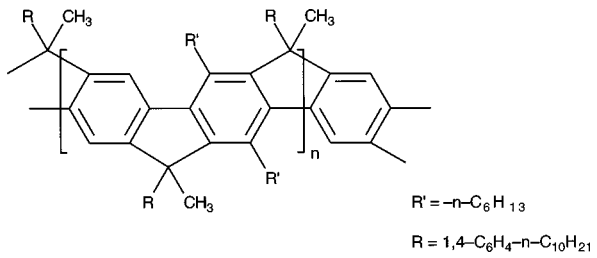

FIG. 1. Structural formula of the ladder-type poly(para-phenylene), MeLPPP.

is shown in Fig. 1. The rigidity of the polymer and careful synthetic protocol result in a particularly narrow distribution of effective conjugation lengths, and consequently optical properties showing electronic transitions with narrow linewidths and well-resolved vibronic structure. The polymer is nevertheless readily soluble in chloroform and toluene, forms high-quality (low scattering) optical films upon spin coating or drop casting, and also has a relatively high photoluminescence efficiency[6] (approximately 80% in solution, 25% in solid films).

While experimental and quantum-chemical extrapolation studies on oligomers can yield significant insight into the electronic properties of the corresponding polymers in the long oligomer limit, it is not easy to synthesize and purify well-defined long oligomers, because of their poor solubility and thermal stability. Also, when moderately long oligomers are coupled to form longer oligomers, there is the potential problem of incomplete conjugation throughout the oligomer, since the selectivity of the α-α or 1,4 (para) coupling at the terminal carbon atoms can be lower as the oligomers being coupled become longer. Studies of the optical and electronic properties of methyl substituted ladder-type poly(paraphenylene) (MeLPPP) therefore offer the advantage of observing sharp molecular spectra, such as that evident in the well-ordered polydiacetylenes, while nevertheless investigating the properties of a ''typical'' soluble, highly fluorescent conjugated polymer containing aromatic rings; in this respect MeLPPP has much in common with PPV or polythiophene and their derivatives. In this study we use the techniques of electroabsorption and two-photon photoluminescence excitation (PLE) spectroscopy to obtain quantitative information on the excitonic states in MeLPPP.

II. EXPERIMENTAL DETAILS

MeLPPP was synthesised using the Suzuki reaction, as described elsewhere.[7] The polymer was dissolved in chloroform at a concentration of 9 mg/ml, then filtered to remove particles with a diameter greater than 0.2 μm. Devices for electroabsorption measurements were prepared using 1-mm thick Herasil quartz substrates with interdigitated evaporated chrome electrodes of separation 160 μm, upon which the polymer layer was deposited either by spin coating or drop casting followed by slow evaporation. Optical absorption measurements of electrode-free areas of the devices were made at room temperature and 80 K, using a Lambda-9 UV-Vis spectrometer and also a McPherson vacuum spectrometer. Absorption measurements of a series of various concentrations of MeLPPP in chloroform were also measured at 300 K using the Lambda-9 UV-visible spectrometer. For the electroabsorption measurements, the device was mounted in an optical access cryostat, within the path of premonochromated light from a Spex 500M single grating 0.5-m monochromator, with a 50-W xenon lamp as light source. The monochromator gratings were ruled with 1200 lines/mm, width 10 cm, blazed at 500 nm to cover the visible region and at 300 nm for the ultraviolet region. The incident light was polarized by a calcite polarizer before being focused onto the device by a quartz concave mirror of focal length 15 cm. A sinusoidal voltage amplified to peak amplitudes of up to 2000 V was applied to the interdigitated electrodes to achieve fields of up to 10^5 V/cm. The transmitted light was focused onto an Oriel photomultiplier tube with S20 characteristic, operating at -600 V. The dc and ac components of the output were detected simultaneously using respectively a Keithley 2000 multimeter and Stanford SR830 lock-in amplifier referenced to the second harmonic of the modulation voltage, with sinusoidal triggering. The phase of the lock-in amplifier was optimized to give the largest positive $\Delta\alpha$ signal, so as to have the same polarity as the first derivative of absorption. A microcomputer controlled the monochromator drive and read in the ac and dc components (ΔT and T) from the lock-in amplifier and multimeter respectively, calculating the ratio $\Delta T/T$, taking into account measurement of background (offset) values and allowing sufficient averaging and delays to follow the true electroabsorption signal and reduce the noise to an acceptable level.

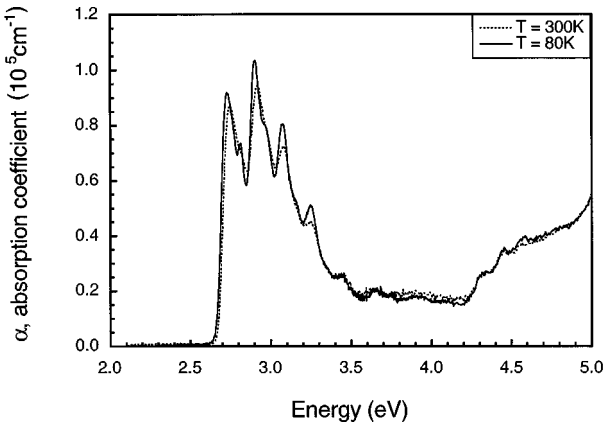

FIG. 2. Absorption spectrum of an MeLPPP thin film at 300 and 80 K.

III. EXPERIMENTAL RESULTS

A. Absorption spectra

The absorption spectra of undiluted cast films of MeLPPP at 300 and 80 K are shown in Fig. 2, and for dilute solution in chloroform in Fig. 3. In contrast with many conjugated polymers, the spectra show particularly well-resolved vibronic structure with remarkably narrow linewidths, both in solution [$\sigma = 30$ meV (the full width at half maximum 70 meV) at 300 K] and in the solid state [$\sigma = 40$ meV (the full

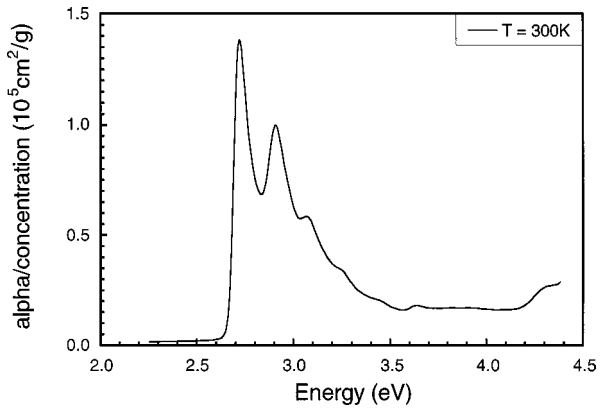

FIG. 3. Absorption spectrum of MeLPPP in a dilute solution in $CHCl_3$.

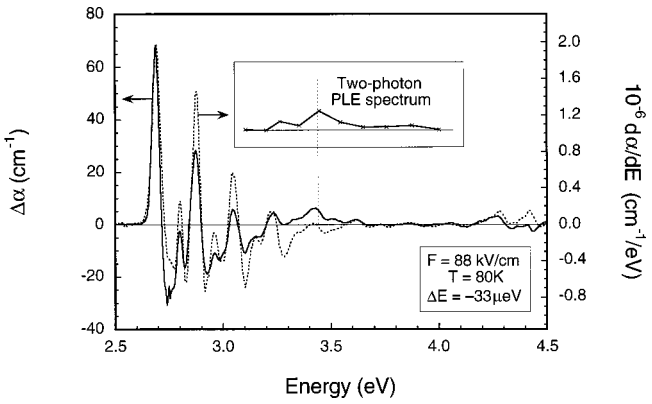

FIG. 4. Electroabsorption spectrum measured at 80 K (**E**∥**F**) and comparison with the first energy derivative of the absorption coefficient at 80 K. The location of the two-photon mA_g state is also indicated for comparison with the broad underlying feature in electroabsorption between 3.2 and 3.6 eV.

width at half maximum 95 meV) at 300 K]. There is a very small blueshift (30 meV) from dilute solution to solid-state films, and also a very small redshift of the solid state spectra with decreasing temperature (20-meV redshift on cooling from 300 to 80 K). These three characteristics (narrow linewidth, small solvatochromism, small thermochromism) are in marked contrast with many conjugated polymers. For poly (-methoxy, 5-ethyl (2-hexyloxy)para-phenylenevinylene) (MEH-PPV), the corresponding thermochromic redshift of the absorption spectrum[8] upon cooling from 300 to 80 K is greater than 100 meV. The low degree of thermochromism and solvatochromism for MeLPPP can be understood if the geometry is indeed locked into a planar structure by the five-membered rings which bridge adjacent phenylene rings. This hinders torsions and librations, thus resulting in a particularly narrow distribution of effective conjugation lengths and hence the narrow linewidths observed.

The 0-0 electronic transition is located at 2.728 ± 0.004 eV for the 80-K absorption spectrum. The absorption spectra both in solution and in solid films show evidence of a dominant vibronic progression corresponding to a phonon energy of approximately 0.177 ± 0.004 eV. However, the peaks are rather asymmetric, usually consisting of a sharp rise and narrow width on the low-energy side, followed by a more gradual fall on the higher-energy side. Furthermore, the first derivative of the absorption spectra both in solution and in films show evidence for an additional phonon frequency at approximately 0.080 ± 0.004 eV, which is resolved as a shoulder and a peak in the absorption spectrum at 80 K (Fig. 2). At higher energy, a further excitonic transition at approximately 4.30 eV appears, also accompanied by a vibronic progression. This is seen clearly in the absorption spectrum and its derivatives. For this higher lying transition, a phonon with energy 0.11–0.12 eV dominates.

B. Electroabsorption spectra

The 80-K electroabsorption spectrum of MeLPPP is shown in Fig. 4. The room-temperature spectrum is similar, although the vibronic structure is less well resolved. For applied fields up to 10^5 V/cm, the electroabsorption resembles the first derivative of the linear absorption spectrum across the entire spectral range from 2.6 to 4.3 eV except for a region between 3.2 and 3.6 eV, where there is a significant discrepancy, apparently due to a broad but weak underlying feature, which is absent in the one-photon absorption spectrum. Note that the broad underlying feature agrees well with the position of the peak in the two-photon PLE spectrum, also shown in Fig. 4.

A further discrepancy which one observes in Fig. 4 is that the relative intensities of the vibronic peaks of the electroabsorption spectrum decrease much more steeply with increasing vibronic quantum number than for the first derivative of absorption. This means that we do not simply observe a rigid redshift of the 0-0 singlet transition together with its vibronic replica. We later propose an explanation for this discrepancy. Qualitatively similar behavior was observed by Meinhardt *et al.*,[9] although the reduced disorder and correspondingly narrower spectral linewidths in the material which we investigate here have allowed better resolution of the vibronic structure. We also investigate the nature of the discrepancy in the region 3.2–3.6 eV in greater detail.

Between 3.7 and 4.2 eV, the electroabsorption spectrum is completely featureless. At approximately 4.33 eV, a weak feature is observed, which corresponds closely in energy with a peak in the first derivative of the linear absorption spectrum in this region, although the 0-1 and 0-2 vibronic replicas which appear in the first derivative of absorption could not be clearly resolved in electroabsorption, perhaps due to lower transmitted intensity of the probe beam in the ultraviolet.

Comparison of electroabsorption spectra for light polarized parallel and perpendicular to the applied electric field yielded a value of $\Delta\alpha(E\|F)/\Delta\alpha(E\perp F)$, close to 3:1, consistent with an isotropic distribution of dipoles in three dimensions or within the plane of the film [Eq. (4)]. The entire electroabsorption spectrum scales quadratically with the applied field.

IV. ANALYSIS

A. Absorption spectra

In dilute solution, we observe the 0-0 absorption line at 2.725 ± 0.004 eV. By extrapolating the energy of the 0-0 absorption line measured in solution for the trimer, pentamer, and heptamer,[10] plotted against the reciprocal of number of benzene rings, we estimate an effective conjugation length of 14 ± 1 phenylene rings for the MeLPPP used in this work. Due to the very small spectral shift between solution and solid state, the effective conjugation length should be similar in the solid state. The number-averaged molecular weight for MeLPPP corresponds to around 50–60 phenylene rings along the backbone or a molecular length of around 300 Å.[11,12]

The same phonon frequencies are observed both in low-temperature absorption and electroabsorption spectra. Analysis of the solid state spectra suggest that both modes couple similarly strongly, with Huang-Rhys parameters of 0.86 ± 0.05 for the phonon at 0.177 eV, and 0.72 ± 0.05 for the phonon at 0.080 eV. However, although these frequencies reproduce the positions of all peaks and points of inflection in the solid state spectra, the agreement with the intensities of the higher vibronic peaks is less satisfactory, perhaps be-

cause of anharmonicity of the vibronic potential. Note that the phonon at 0.177 eV (1420 cm^{-1}) is in good agreement with a skeletal C=C stretch mode calculated[13] for planarized LPPP, albeit without phenyl side groups. Note that the phonon at 0.080 eV is not apparent in the low temperature photoluminescence spectra of MeLPPP,[14] suggesting that it couples quite strongly to the $1B_u$ excited state but only weakly to the ground state.

The absorption spectra in solution and in thin films differ in the relative intensities of the vibronic peaks accompanying the low-energy singlet transition, the 0-0 peak dominating in solution, while the 0-1 peak appears to dominate in the undiluted thin film. For materials whose spectra have a very narrow linewidth, it has been noted[15] that the measured absorption spectrum of the solid film may underestimate the oscillator strength of the 0-0 transition because of large changes in refractive index or reflectivity of the polymer at the absorption edge. The imaginary part of the relative permittivity, ε_2, is a more fundamental optical property of the material. The absorption coefficient, α is related to ε_2 by the equation, $\alpha=\omega\varepsilon_2/nc$, where $\hbar\omega$ is the photon energy, n is the refractive index, and c is the speed of light. In dilute solution, the absorption spectrum of the polymer should therefore be more representative of the true absorption spectrum of the material, since the refractive index of the dilute solution will be dominated by that of the solvent, which shows no structure in the visible region.

B. Electroabsorption spectra

1. Broad discrepancy between 3.2 and 3.6 eV

The broad discrepancy between the electroabsorption spectrum and the first derivative of the absorption spectrum suggests that it is due to an optical transition which is forbidden or has a low oscillator strength in the one-photon absorption spectrum. Such transitions include dipole-forbidden transitions between states of the same parity, e.g., $mA_g \leftarrow 1A_g$, charge-transfer transitions or weak absorptions due to aggregates of chain segments.[16] By studying the effects of solid-state dilution and annealing, as well as measuring the two-photon PLE spectrum, we investigate the origin of this transition.

(a) Solid-State dilution. Dilution of the MeLPPP ladder polymer in poly(4-methylstyrene) or polycarbonate at around 5% by weight yielded optically high-quality transparent films with very low scattering, indicating relatively good compatibility and miscibility. However, the detailed microstructure of the diluted films is unknown. The electroabsorption spectra of MeLPPP diluted in each matrix showed a redshift of the 0-0 transition at approximately 2.72 eV by 20 meV at 300 K and 35 meV at 80 K, although the subsequent vibronic replicas were not so greatly redshifted. The electroabsorption spectra of the diluted films of MeLPPP closely resemble those of the neat MeLPPP films. Furthermore, the relative strength of the broad underlying feature (displacement between electroabsorption spectrum and first derivative) in the region of approximately 3.4 eV remains unchanged, suggesting that it is probably not of intermolecular origin.

(b) Annealing. Ladder-type polyphenylenes show evidence of aggregate formation in the solid state[17] and especially upon annealing.[18] This is apparent as a broad emission

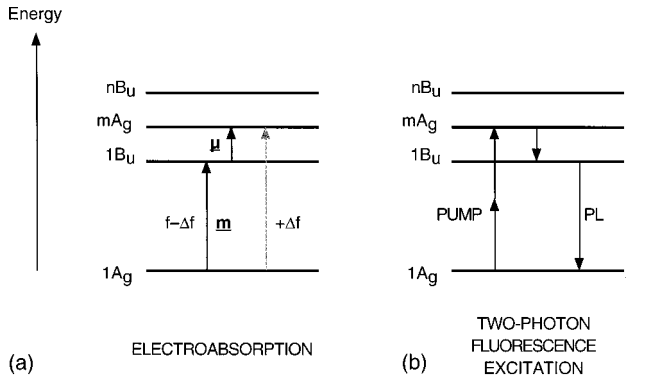

FIG. 5. Energy-level diagram showing the coupling of states by the electric field in electroabsorption (a) together with the transitions involved in the two-photon fluorescence excitation measurements (b).

centered around 2.0 eV and also as a very weak absorption at approximately 2.25 eV,[16] both well below the 0-0 singlet exciton transition. Such broad aggregate emission is not so pronounced in MeLPPP films.[14] The methyl substituent in MeLPPP results in greater steric hindrance of the side chains, and probably a greater interchain separation. However, upon annealing at 150 °C for 8 h under vacuum, a broad feature appears below 2.0 eV in the photoluminescence spectrum, and is assigned to emission from aggregates.[19] However, for our devices, neither the absorption spectrum nor the electroabsorption spectrum shows any change upon annealing the device at 150 °C for 12 h under vacuum. This is further evidence that the optical transitions observed are primarily of an intrachain nature.

(c) Two-photon photoluminescence excitation spectroscopy. Strong two photon absorption has been observed in this region in MeLPPP at 800 nm (Ref. 20) (corresponding to a one-photon energy of 3.1 eV), although, until now, no detailed spectral information on the shape of the two-photon absorption of this material was available in the literature. We measured the two-photon PLE spectrum of MeLPPP in order to obtain the lineshape of a higher-lying gerade excited state (mA_g), rendered partially allowed in the presence of an electric field. A transition from the ground state ($1A_g$) to the gerade state (mA_g) can be achieved by absorption of two photons as indicated in Fig. 5. The two-photon PLE spectrum is shown as an inset in Fig. 4. Our two-photon studies of MeLPPP will be described in detail elsewhere.[21] The main point to note is that the two-photon PLE spectrum shows a maximum at approximately 3.45 ± 0.10 eV, in close agreement with the location of the broad underlying feature.

2. Linear and quadratic Stark effects

Close agreement with the first derivative of absorption, together with the observed proportionality to the square of the applied field, is indicative of a quadratic Stark shift of a singlet exciton [Eq. (1)]. The energy shift is related to the polarization energy,[22] where p is the polarizability of the $1B_u$ exciton and μ_{ij} is the dipole moment between the $1B_u$ exciton and other states (e.g., between $1B_u$ and mA_g),

$$\Delta E_i=\sum_{i\neq j}\left(\frac{|\mu_{ij}\mathbf{F}|^2}{E_i-E_j}\right)=\frac{1}{2}pF^2=\frac{4\pi\varepsilon_0}{2}p_{\mathrm{CGS}}|F_{\mathrm{SI}}|^2, \quad (1)$$

where the subscripts CGS and SI denote the respective metric systems in which the polarizability p and field strength F are expressed. The rigid shift of the exciton results in a contribution following the line shape of the first derivative of absorption. In addition to causing a redshift of the singlet exciton, the quadratic Stark effect also predicts a transfer of oscillator strength to a higher lying excited state in the presence of an applied electric field, as indicated in Eq. (2):

$$\frac{\Delta f_{ij}}{f_{ij}} = \frac{|\mu_{ij}\mathbf{F}|^2}{(E_i - E_j)^2}. \tag{2}$$

The transfer of oscillator strength can be approximated by a contribution following the absorption line shape, but with a negative sign. This is also shown schematically in Fig. 5 for transfer of oscillator strength to a higher-lying mA_g state.

For most disorded conjugated polymers, it is often the case that the electroabsorption spectrum can be better described by a superposition of both the quadratic Stark effect, [Eqs. (1) and (2)], and the nonzero second-order term of the linear Stark effect [Eq. (3)]:

$$\Delta\alpha = \left\langle \frac{d\alpha}{dE}\Delta E \right\rangle + \left\langle \frac{1}{2}\frac{d^2\alpha}{dE^2}(\Delta E)^2 \right\rangle \quad \text{where} \quad \Delta E = \mathbf{m}\cdot\mathbf{F}. \tag{3}$$

The dipole moment **m** can be due to permanent dipoles due to defects or charge-transfer states but can also be understood in terms of dipoles induced by disorder as a result of a subtle asymmetry of the charge density along a conjugated segment when the potentials at either end of the segment are unequal.[23,24] The first-order term of the linear Stark effect vanishes for an isotropic distribution of molecules. The second-order term remains even after averaging over all chain orientations and contributes a second-derivative line shape.

We tried to fit the experimental spectra to the expression in Eq. (4):

$$\begin{aligned}\Delta\alpha(\mathbf{E}\|\mathbf{F}) &= \frac{3}{5}\left[\frac{d\alpha}{dE}\frac{|\mu_{ij}|^2|\mathbf{F}|^2}{E_j - E_i}\right] - \frac{3}{5}\left[\alpha\frac{|\mu_{ij}|^2|\mathbf{F}|^2}{(E_j-E_i)^2}\right] \\ &\quad + \frac{3}{5}\left[\frac{1}{2}\frac{d^2\alpha}{dE^2}|\mathbf{m}|^2|\mathbf{F}|^2\right], \\ \Delta\alpha(\mathbf{E}\perp\mathbf{F}) &= \frac{1}{5}\left[\frac{d\alpha}{dE}\frac{|\mu_{ij}|^2|\mathbf{F}|^2}{E_j - E_i}\right] - \frac{1}{5}\left[\alpha\frac{|\mu_{ij}|^2|\mathbf{F}|^2}{(E_j-E_i)^2}\right] \\ &\quad + \frac{1}{5}\left[\frac{1}{2}\frac{d^2\alpha}{dE^2}|\mathbf{m}|^2|\mathbf{F}|^2\right].\end{aligned} \tag{4}$$

We consider only the states $1A_g$ and $1B_u$ and a higher-lying mA_g state. From left to right, the terms represent (i) the energy redshift of the $1B_u$ exciton due to the quadratic Stark effect, (ii) the transfer of oscillator strength from the $1B_u$ exciton to a higher mA_g exciton (due to field-induced mixing of the $1B_u$ and mA_g states within the quadratic Stark effect), and (iii) the nonvanishing contribution of the second-order linear Stark effect due to defect-induced or disorder-induced dipoles.

The factors $\frac{3}{5}$ (for $E\|F$) and $\frac{1}{5}$ (for $E\perp F$) arise from orientational averaging over a three-dimensional isotropic distribution of segment orientations.[22,24] The expressions within the brackets are otherwise the corresponding terms for the case in which applied electric field **F**, optical electric field **E** and chain segment are all exactly parallel or antiparallel to each other, as can be arranged for isolated one-dimensional chains of polydiacteylenes.

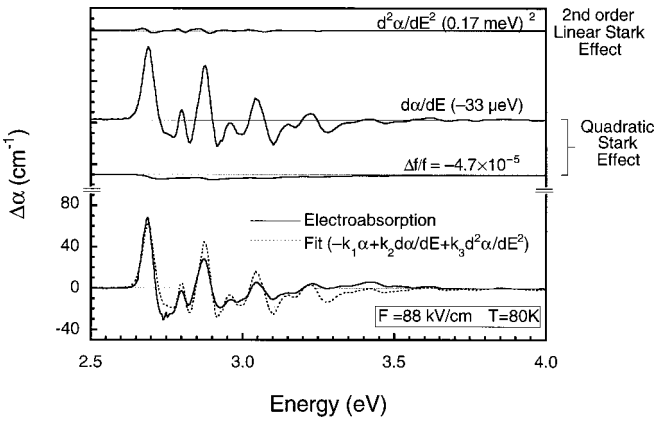

FIG. 6. Comparison of the experimental electroabsorption spectrum at 80 K with a fit which includes contributions of the absorption coefficient α and the first derivative $d\alpha/dE$, (corresponding, respectively, to a loss of oscillator strength and a redshift, due to the quadratic Stark effect) and the second derivative $d^2\alpha/dE^2$ (the second-order term in the linear Stark effect due to dipoles caused by disorder). Note that the contribution from the first derivative dominates, although the relative intensities of the vibronic peaks do not agree with the fit.

Note that there are actually only two parameters in the fit, namely, μ_{ij} and **m**. The first two terms differ only by a factor of the energy separation of the $1B_u$ and mA_g states, which can be determined independently from two-photon spectroscopy.

The results of the best fit to Eq. (4) are shown in Fig. 6. However, note that the discrepancy in the relative heights of the vibronic peaks and in the region around 3.2–3.6 eV is still present.

3. Discrepancy in the relative heights of the vibronic peaks

The relative height of the vibronic peaks of the singlet exciton decrease much more rapidly with increasing vibrational quantum number for the electroabsorption spectrum than for the first derivative of absorption. It has already been noted[15] that the experimental values of the intensity of the 0-0 transition determined from α or $d\alpha/dE$ may be underestimated compared with that obtained from ε_2. An example is the case of a polymethine dye with a very narrow linewidth in the ε_2 spectrum,[25] for which the absorption spectrum is much broader, with a highly asymmetric tail falling off much more gradually at higher energy. By measurements of the Brewster angle and Kramers-Kronig analysis of the reflection spectra, we can deduce the spectral dependence of the refractive index, $n(E)$. The first derivative of ε_2 is given by $d(\varepsilon_2)/dE = (c/\omega)[\alpha(dn/dE) + n(d\alpha/dE)]$. For our spectra, we note that the latter term $n\,(d\alpha/dE)$ is greater than the former term α, (dn/dE) by a factor of about 9. The change in refractive index can therefore only partially explain the discrepancy. Furthermore, comparison of the electroabsorption signal with the derivatives of $n\,\alpha$ or ε_2 does

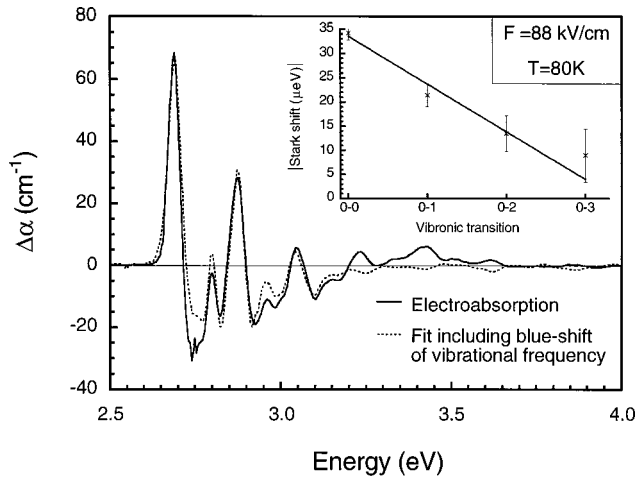

FIG. 7. Comparison of the experimental electroabsorption spectrum at 80 K with a fit based on the derivatives of absorption, as in Fig. 6, together with a contribution from a small blueshift of the vibrational frequencies in the presence of the field. Note that the relative heights of the vibronic peaks are now much better reproduced in the fit. The inset shows the apparent Stark shift determined for each of the vibronic peaks, from which the true Stark shift and the vibrational blueshift can be determined.

not yield closer agreement and only changes the relative heights of the vibronic peaks by around 10%.

As an alternative explanation for the discrepancy in the relative heights of the vibronic peaks, we consider that the electric field might also modify the vibrational energies as well as the electronic transition energies. A slight stiffening of the chains in the presence of an electric field would give rise to a small blueshift of the vibrational energies, increasing with increasing quantum number. This effect should not affect the 0-0 transition but would increasingly oppose the redshift due to the quadratic Stark effect for the higher vibronic peaks. Since the ratios between the heights of the vibronic peaks in the electroabsorption spectra do not change with field strength, the vibrational blueshift must have the same quadratic field dependence as does the quadratic Stark effect. In Fig. 7, we have included a vibrational blueshift in the derivative fit. We assume that the fit must hold for the 0-0 transition, since the vibrational blueshift should not affect this transition and since we have established that the effects of changes in reflectivity or refractive index cannot explain the discrepancy in the intensity of the 0-0 transition in this case. In Eq. (5), we describe the total change of absorption therefore as arising from an electronic contribution (a rigid redshift of the 0-0 transition and its vibronic replica due to the quadratic Stark effect) and a vibronic contribution which scales with vibrational quantum number and also follows the first derivative line shape:

$$\Delta\alpha = \frac{d\alpha}{dE}(\Delta E_{\mathrm{el}} + n_{\mathrm{vib}}\delta E_{\mathrm{vib}}). \tag{5}$$

In order to avoid abrupt steps in the fit of Fig. 7, we represent the vibrational quantum number n_{vib} by a continuous function, using the expression in Eq. (6).

$$n_{\mathrm{vib}} \approx (E - E_{0-0})/\Delta E_{\mathrm{vib}}. \tag{6}$$

In no way do we intend to suggest that n_{vib} is not discrete. The intention is only to show that a small vibrational blueshift of $\delta E_{\mathrm{vib}}(F^2)$ of 10 μeV per 177 meV phonon at a field strength of 88 kV/cm is sufficient to produce a much better agreement in the relative heights of the major vibronic peaks. Note also that even after the vibrational correction, a broad underlying discrepancy at approximately 3.45 eV remains, although this is to be expected if the mA_g state lies at this energy.

The mA_g state may have a different curvature from that of the $1B_u$ exciton or the $1A_g$ ground state. Since the eigenstates in the presence of the electric field are derived by mixing the eigenstates in the absence of the field, it is quite plausible that a mixing of the vibronic states should also occur, and that a change of the vibrational frequency could be observed. Such a small change is usually close to the experimental uncertainty in vibrational energies, but can apparently be detected by the sensitivity of electroabsorption measurements for a material with narrow linewidths. It is interesting to note, from Figs. 6 and 7, that the fractional transfer of oscillator strength is of the same order of magnitude as the inferred fractional change of the phonon frequency at the same field strength ($\delta\omega/\omega \approx 5\times10^{-5}$ at $F = 88$ kV/cm).

Liess *et al.*[26] presented a theoretical model in which they attempted to deconvolute the electroabsorption spectra of disordered conjugated polymers within the inhomogeneously broadened 0-0 transition. As a consequence, they concluded that the polarizability should be greater for longer conjugated segments toward the lower-energy tail of the energetic distribution. However, their model does not readily explain the case of the polydiacetylene 4-BCMU, for which increasing levels of structural disorder barely alter the polarizability,[23,24] although disorder has a marked effect on the optical properties (e.g., increasing linewidth, or a blueshift of electronic transitions for shorter lengths of conjugated segments between interruptions), and introduces an increasing component of second-derivative line shape. We comment that an increase of the vibrational frequencies quadratically with the field strength may also have general validity for understanding the electroabsorption lineshape of more disordered conjugated polymers. Note, however, that for well-ordered single chains of polydiacetylenes 4-BCMU and 3-BCMU,[27] no vibrational shift can be inferred—although for these chains, the coherence length is presumably much longer, since the Franz-Keldysh effect can be observed in such materials and the electron-phonon coupling is therefore weaker.

4. Quantitative analysis of the electroabsorption spectra

In Fig. 7, we show the improved fit to the electroabsorption spectra at 80 K due to the contributions of the zero, first, and second derivative line shapes (quadratic and second-order linear Stark effects) and including an increase of the vibrational frequencies as just described. It is evident in Fig. 6 that the dominant contribution arises from the first derivative of absorption, for which a redshift of 33 μeV is measured, corresponding to a polarizability of 2060 Å^3. The same fit redshift of 33 μeV also gives a good fit to the room-temperature spectrum. Taking the gap between the mA_g and $1B_u$ states to be approximately 0.73 eV (the center of the

discrepancy or the two-photon PLE peak at 3.45 eV minus the 0-0 transition of the $1B_u$ exciton at 2.72 eV), we calculate that a dipole moment μ of $7.2e$Å (34D) couples the $1B_u$ and mA_g excitons. The charge separation is significantly less than the effective conjugation length of 14–15 phenylene rings (≈50 Å). The values of the polarizability and dipole moment are nevertheless considerably lower than those obtained for chains of the polydiacetylenes 4-BCMU and 3-BCMU isolated within single-crystal matrices of the monomer. (7120 Å^3, $12e$Å≈58 D) for 3-BCMU and (6480 Å^3, $11.3e$Å≈54 D) for 4-BCMU.[27]

V. DISCUSSION

A. Influence of disorder and defects on the line shape of electroabsorption

It is perhaps worth comparing the electroabsorption spectra of MeLPPP with those of the polydiacetylene, 4-BCMU, in which the degree of structural order was systematically varied,[24] from isolated chains in a single crystal of the monomer to spin-coated films. For isolated 4-BCMU chains within the single crystal of the monomer, the electroabsorption spectrum is dominated by the first derivative of absorption, i.e., the quadratic Stark effect, and the linewidth is extremely narrow, (the full width at half maximum is approximately 10 meV at 77 K). For 4-BCMU, polymer single crystals removed from the monomer substrate show broader linewidths [the full width at half maximum (FWHM) 80 meV at 77 K] than the isolated chains and also an increased contribution of the second derivative line shape. For the highly disordered chains within the spin-coated films of 4-BCMU, the contribution of the second derivative line shape dominates and the linewidth is even broader (the FWHM is approximately 155 meV at 300 K) and highly asymmetric, with a broad tail on the lower-energy side.

For highly ordered materials, such as single-crystalline polydiacetylenes, improved PPV,[28] and, to some extent, β-carotene,[29,30] the electroabsorption spectrum agrees quite closely with the first derivative of absorption, although, even for β-carotene, a significant component following the second derivative line shape is required for a good fit. For less well-ordered materials showing broad absorption spectra with a poorly resolved vibronic structure, the contribution with the second derivative line shape increases and can even be the dominant contribution, e.g., for spin-coated films of the polydiacetylene 4-BCMU. However, intrachain order alone is not the only factor influencing the relative influence of first and second derivative contributions; the electroabsorption spectrum of poly(3-octylthiophene)[31] is dominated by a first derivative response, while the electroabsorption spectrum of poly(thienylenevinylene)[32] closely follows the second derivative, although both polymer samples have very similar absorption spectra, similar resolution of vibronic transitions and similar linewidths—but perhaps differ in the concentration of defect-induced dipoles. For most materials studied to date, the contribution following the second derivative is not negligible, and the additional parameter **m** introduced in the fit has meant that it has not previously been possible to resolve such a small fractional change of the phonon frequencies of ($\delta\omega/\omega \approx 5\times10^{-5}$ at $F=88$ kV/cm) in most other conjugated polymers.

In the case of the electroabsorption spectra of cast films of MeLPPP, it is clearly the first derivative line shape which dominates, while the contribution of the second derivative is much weaker. This is shown in Fig. 6. We observed no qualitative differences between spin-coated and cast films. Furthermore, the linewidth (the FWHM is approximately 35 meV at 77 K and 45 meV at 300 K) is much narrower than that of the spin-coated films of 4-BCMU, and is indeed narrower than that of polymer single crystals of 4-BCMU removed from the monomer substrate. Clearly MeLPPP retains a high degree of intrachain order, even in solution. In MeLPPP, the intrachain order is achieved by directly planarizing the backbone, whereas for the polydiacetylene 4-BCMU, planarization and suppression of twisting motions (torsions and librations) rely upon the crystallinity and hydrogen bonding between urethane side groups at some distance from the main chain. The intrachain geometry for 4-BCMU is therefore less ordered in the spin-coated films, while for MeLPPP the intrachain rigidity persists. Furthermore, the weak contribution of the second derivative line shape also attests to a very low concentration of permanent dipole moments and high chemical purity of MeLPPP.

B. Energy levels

The transition to the mA_g state, determined from the two-photon PLE spectrum, has an energy approximately 1.25 times that of the 0-0 singlet exciton transition ($1B_u \leftarrow 1A_g$). A very similar value was obtained for PPV; using two-photon PLE spectroscopy, Baker, Gelsen, and Bradley[33] determined that the mA_g state in PPV lies at 2.95 eV, while the $1B_u$ exciton lies at 2.36 eV for (improved) PPV (Ref. 3); the ratio of the transition energies for mA_g and $1B_u$ states, in the case of PPV,[1] then also around 1.25. In thin films of polydiacetylenes, transitions to the mA_g state have been observed[34,35] at 1.2–1.6 times the energy of the transition to the $1B_u$ state, although it should be noted that for single crystals of the polydiacetylene 4-BCMU, a much stronger response is observed in electroabsorption at around 1.3 times the transition energy of the singlet, together with field-dependent broadening. In that case, the intensity of the signal relative to that of the singlet was greater than that which could be attributed to a transfer of oscillator strength, $\Delta f/f$ to the forbidden exciton and the transition has instead been attributed to the Franz-Keldysh effect of the continuum. Experimental[36] and theoretical[37] work on short oligoenes indicated that the lowest A_g state ($2A_g$) may lie below the $1B_u$ state and thus account for the low photoluminescence yields. Electroabsorption studies on β-carotene[30] located the $1B_u$ exciton at 2.47 eV. A weaker transition at 1.77 eV was attributed to the $2A_g$ exciton, while a higher-lying mA_g exciton at around 3.2 eV dominates the dipole coupling to the $1B_u$ state and accounts for the net Stark redshift of the $1B_u$ exciton. If the $2A_g$ state were to couple more strongly to the $1B_u$ exciton than the higher-lying mA_g exciton, one would expect a net blueshift rather than a net redshift. The ratio of the transition energies $E(mA_g)/E(1B_u)$ is again around 1.3 for β-carotene.

The response which we observe in electroabsorption shows no field-dependent broadening up to fields of 88 kV/cm. The line shape and intensity are consistent with transfer

of oscillator strength to a forbidden mA_g exciton. It is likely that the feature which we observe in electroabsorption and two-photon PLE spectra around 3.45 eV (1.27 times the $1B_u$ transition energy) is indeed the mA_g state (or several closely spaced states) and is the nearest level which couples to the $1B_u$ exciton which can explain the quadratic Stark effect observed. It is interesting to note that the energetic position of the one-photon-forbidden transition to an mA_g state (approximately 3.4 ± 0.2 eV) lies only slightly below the threshold energy (3.85 ± 0.10 eV) determined for intrinsic photoconduction[38] in MeLPPP. In the surface cell geometry, the photoconductivity quantum yield follows closely the absorption spectrum due to the $1B_u$ exciton and its vibronic progression, then shows a monotonic rise with energy above a threshold energy of 3.7 ± 0.1 eV. Calculations[39] on long one-dimensional loops of 800 carbon atoms indicate that both the higher-lying mA_g state and the continuum lie close together and approximately 1.2–1.3 times higher than the $1B_u$ excitonic transition energy when Coulomb interactions are taken into account ($U/V \approx 3$).

VI. CONCLUSIONS

Despite being a readily soluble conjugated polymer, the electroabsorption spectra of solution-cast films of MeLPPP show remarkably narrow linewidths and close agreement with the first derivative of absorption, while the contribution of the second derivative is much smaller. This indicates that the distribution of conjugation lengths in this material is particularly narrow, and that disorder-induced dipole moments play an almost negligible role in this material, although the coherence length is still not sufficiently long to allow observation of a Franz-Keldysh effect in MeLPPP. In this respect, MeLPPP is intermediate between high quality polydiacetylene single crystals and disordered conjugated polymers. We interpret the spectra in terms of a redshift of the 0-0 transition and its vibronic replica due to the quadratic Stark effect, together with an increasing blueshift of the higher-lying vibronic peaks due to a small increase of the vibrational energy in the presence of the field, the vibrational blueshift also having a quadratic field-dependence. At an energy approximately 1.25 times that of the $1B_u$ exciton, we locate the mA_g forbidden exciton, whose interaction with the $1B_u$ exciton in the presence of an applied field is responsible for the observed quadratic Stark effect. A polarizability of 2060 Å^3 and a dipole moment of $7.2e$Å (34D) is calculated for the $1B_u$ exciton.

ACKNOWLEDGMENTS

For financial support, we thank the Training and Mobility of Researchers Programme of the European Commission, ''SELOA'' (Synthetic Electroactive Organic Architectures) (Contract No. ERBFMRX-CT96-0083), the Deutsche Forschungsgemeinschaft (Sonderforschungsbereich 383), and the Fonds der Chemischen Industrien. We also thank Professor K. Müllen for a fruitful collaboration and Dr. H. Mell for assistance with the preparation of the interdigitated electrodes.

[1] U. Rauscher, L. Schutz, A. Greiner, and H. Bässler, J. Phys.: Condens. Matter **1**, 9751 (1989).
[2] R. Mahrt, J. P. Yang, A. Greiner, H. Bässler, and D. D. C. Bradley, Makromol. Chem., Rapid Commun. **11**, 415 (1990).
[3] S. Heun, R. F. Mahrt, A. Greiner, U. Lemmer, H. Bässler, D. A. Halliday, D. D. C. Bradley, P. L. Burn, and A. B. Holmes, J. Phys.: Condens. Matter **5**, 247 (1993).
[4] K. Pichler, D. A. Halliday, D. D. C. Bradley, P. L. Burn, R. H. Friend, and A. B. Holmes, J. Phys.: Condens. Matter **5**, 7155 (1993).
[5] L. Sebastian and G. Weiser, Phys. Rev. Lett. **46**, 1156 (1981).
[6] J. Stampfl, S. Tasch, G. Leising, and U. Scherf, Synth. Met. **71**, 2125 (1995).
[7] U. Scherf, A. Bohnen, and K. Müllen, Makromol. Chem., Macromol. Chem Phys. **193**, 1127 (1992).
[8] M. G. Harrison, J. Grüner, and G. C. W. Spencer, Phys. Rev. B **55**, 7831 (1997).
[9] G. Meinhardt, A. Horvath, G. Weiser, and G. Leising, Synth. Met. **84**, 669 (1997).
[10] J. Grimme, M. Kreyenschmidt, F. Uckert, K. Müllen, and U. Scherf, Adv. Mater. **7**, 292 (1995).
[11] J. Grimme and U. Scherf, Macromol. Chem. Phys. **197**, 2297 (1996).
[12] W. Graupner, S. Eder, M. Mauri, G. Leising, and U. Scherf, Synth. Met. **69**, 419 (1995).
[13] L. Cuff and M. Kertesz, J. Phys. Chem. **98**, 12 223 (1994).
[14] B. Schweitzer, G. Wegmann, H. Giessen, D. Hertel, H. Bässler, R. F. Mahrt, U. Scherf, and K. Müllen, Appl. Phys. Lett. **72**, 2933 (1998).
[15] B. Reimer, H. Bässler, J. Hesse, and G. Weiser, Phys. Status Solidi B **73**, 709 (1976).
[16] A. Köhler, J. Grüner, R. H. Friend, K. Müllen, and U. Scherf, Chem. Phys. Lett. **243**, 456 (1995).
[17] R. F. Mahrt, T. Pauck, U. Lemmer, U. Siegner, M. Hopmeier, R. Hennig, H. Bässler, E. O. Göbel, P. H. Bolivar, G. Wegmann, H. Kurz, U. Scherf, and K. Müllen, Phys. Rev. B **54**, 1759 (1996).
[18] J. Huber, K. Müllen, J. Salbeck, H. Schenk, U. Scherf, T. Stehlin, and R. Stern, Acta Polym. **45**, 244 (1994).
[19] D. Hertel, H. Bässler, U. Scherf, and H. H. Hörhold, J. Chem. Phys. **110**, 9214 (1999).
[20] M. Samoc, A. Samoc, B. Luther-Davies, and U. Scherf, Synth. Met. **87**, 197 (1997).
[21] M. G. Harrison, G. Urbasch, R. F. Mahrt, and H. Bässler (unpublished).
[22] A. Horvath, H. Bässler, and G. Weiser, Phys. Status Solidi B **173**, 755 (1992).
[23] A. Horvath, G. Weiser, G. L. Baker, and S. Etemad, Phys. Rev. B **51**, 2751 (1995).
[24] G. Weiser and A. Horvath, Chem. Phys. **227**, 153 (1998).
[25] L. Dähne, A. Horvath, G. Weiser, and G. Reck, Adv. Mater. **8**, 486 (1996).
[26] M. Liess, S. Jeglinski, Z. V. Vardeny, M. Ozaki, K. Yoshino, Y. Ding, and T. Barton, Phys. Rev. B **56**, 15 712 (1997).
[27] A. Horvath, G. Weiser, C. Lapersonne-Meyer, M. Schott, and S.

Spagnoli, Phys. Rev. B **53**, 13 507 (1996).
[28] D. A. Halliday, P. L. Burn, D. D. C. Bradley, R. H. Friend, O. M. Gelsen, A. B. Holmes, A. Kraft, J. H. F. Martens, and K. Pichler, Adv. Mater. **5**, 40 (1993).
[29] F. Rohlfing, D. D. C. Bradley, A. Eberhardt, K. Müllen, J. Cornil, D. Beljonne, and J. L. Brédas, Synth. Met. **76**, 35 (1996).
[30] F. Rohlfing and D. D. C. Bradley, Chem. Phys. Lett. **277**, 406 (1997).
[31] C. Botta, G. Zhuo, O. M. Gelsen, D. D. C. Bradley, and A. Musco, Synth. Met. **55–57**, 85 (1993).
[32] O. M. Gelsen, D. D. C. Bradley, H. Murata, T. Tsutsui, S. Saito, J. Rühe, and G. Wegner, Synth. Met. **41–43**, 875 (1991).
[33] C. J. Baker, O. M. Gelsen, and D. D. C. Bradley, Chem. Phys. Lett. **201**, 127 (1993).
[34] P. D. Townsend, W. S. Fann, S. Etemad, G. L. Baker, Z. G. Soos, and P. C. M. McWilliams, Chem. Phys. Lett. **180**, 485 (1991).
[35] Y. Tokura, Y. Oowaki, T. Koda, and R. Baughman, Chem. Phys. **88**, 437 (1984).
[36] B. E. Kohler, C. Spangler, and C. Westerfield, J. Chem. Phys. **89**, 5422 (1988).
[37] B. E. Kohler, J. Chem. Phys. **93**, 5838 (1990).
[38] S. Barth, H. Bässler, U. Scherf, and K. Müllen, Chem. Phys. Lett. **288**, 147 (1998).
[39] S. Abe, M. Schreiber, W. P. Su, and J. Yu, Phys. Rev. B **45**, 9432 (1992).